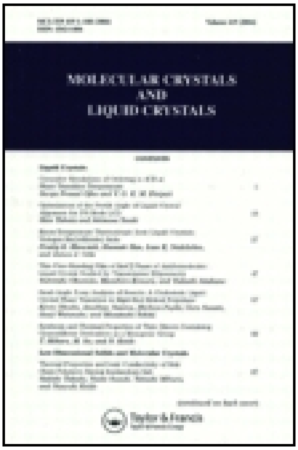

Molecular Crystals and Liquid Crystals

Publication details, including instructions for authors and subscription information:
http://www.tandfonline.com/loi/gmcl20

Organic Solar Cells Incorporating a p-i-n Junction

Masahiro Hiramoto [a], Kouji Suemori [a] & Masaaki Yokoyama [a]

[a] Material and Life Science, Graduate School of Engineering, Osaka University, Yamadaoka, Suita, Osaka, Japan

Version of record first published: 20 Aug 2006

To cite this article: Masahiro Hiramoto, Kouji Suemori & Masaaki Yokoyama (2006): Organic Solar Cells Incorporating a p-i-n Junction, Molecular Crystals and Liquid Crystals, 444:1, 33-40

To link to this article: http://dx.doi.org/10.1080/15421400500374963

Mol. Cryst. Liq. Cryst., Vol. 444, pp. 33–40, 2006
Copyright © Taylor & Francis LLC
ISSN: 1542-1406 print/1563-5287 online
DOI: 10.1080/15421400500374963

Organic Solar Cells Incorporating a *p-i-n* Junction

Masahiro Hiramoto
Kouji Suemori
Masaaki Yokoyama
Material and Life Science, Graduate School of Engineering,
Osaka University, Yamadaoka, Suita, Osaka, Japan

Three-layered organic solar cells incorporating a co-deposited interlayer of fullerene and metal-free phthalocyanine, whose nanostructure was optimized by controlling the substrate temperature during co-evaporation, showed a photo-electric conversion efficiency of 2.5% under illumination with simulated solar light. The three-layered cells were concluded to have a ***p-i-n****-like energetic structure. For the long-term operation, cells should be isolated from air to avoid the ingress of oxygen or water.*

Keywords: co-deposited interlayer; *p-i-n* junction; three-layered organic solar cells

INTRODUCTION

Mixed films of two kinds of organic semiconductors that act as donors and acceptors possess high potential for photocarrier generation [1]. We previously reported *p-i-n* organic solar cells in which the *i*(*intrinsic*)-interlayer is a co-deposited film of organic semiconductors [2–4] after the epoch-making work on organic *p-n* heterojunctions by Tang [5]. Since the nanostructure of co-deposited films is obviously believed to influence the photocurrent generation process, we have tried to control the nanostructure of co-deposited films between phthalocyanine and perylene pigments by varying the substrate temperature during vacuum co-evaporation [6]. On the other hand, co-deposited fullerene (C_{60}) and phthalocyanine (Pc) films have been revealed to possess an extraordinary high photocarrier generation potential [7–12]. Therefore,

Address correspondence to Masahiro Hiramoto, Material and Life Science, Graduate School of Engineering, Osaka University, Yamadaoka, Suita, Osaka 565-0871, Japan. E-mail: hiramoto@chem.eng.osaka-u.ac.jp

we decided to incorporate the nanostructure-controlled C_{60}:Pc co-deposited films into *p-i-n*-type cells.

In this paper, we report three-layered organic solar cells incorporating the nanostructure-optimized C_{60}:Pc co-deposited interlayer. A photo-electric conversion efficiency of 2.5% was observed.

EXPERIMENTAL

C_{60}, metal-free phthalocyanine (H_2Pc), naphthalene tetracarboxylic anhydride (NTCDA, Fig. 2) and Ag counter electrodes were deposited by the vacuum evaporation technique under 1×10^{-3} Pa onto indium tin oxide (ITO) glass substrates pre-treated in an air plasma [13]. Co-deposition was performed by co-evaporation from two-separately-controlled sources. The substrate temperature was controlled using a substrate heater (ULVAC Kiko, Inc.). The photovoltaic properties were measured under simulated solar light (Yamashita Denso, Co. Ltd., YSS-50A); the intensity of the solar light was monitored using a silicon photodiode. Photocurrent action spectra were measured using monochromatic light from 500 W Xenon lamp that had been passed through a monochromator. Usually, measurements were performed under a vacuum conditions (0.1 Pa).

RESULTS AND DISCUSSION

As a first step, we fabricated single-layered cells to optimize the substrate temperature for photovoltaic performance of the C_{60}:H_2Pc. Pronounced enhancement of the magnitude of the short-circuit photocurrent density (J_{sc}) was observed by heating to around +80°C (Fig. 1). The open-circuit photovoltage (V_{oc}) and the fill factor (FF) were enhanced simultaneously. Since the C_{60}:H_2Pc film co-deposited at +80°C has a nanocomposite structure somewhere between crystalline H_2Pc and amorphous C_{60}, which has spatially-separated routes for electrons and holes, the entire bulk of the thick C_{60}:H_2Pc film could contribute to photocurrent generation. Detailed results on the nanostructure control of C_{60}:H_2Pc films were summarized in Ref. [14]. Thus, we decided to incorporate a C_{60}:H_2Pc layer co-deposited at +80°C into a three-layered cells.

The structure of three-layered cells were illustrated in Figure 2. The co-deposited layer was sandwiched between *n-type* NTCDA and *p-type* H_2Pc. Thick NTCDA, which is transparent throughout the visible region, also acts as a protection layer against diffusion of the vacuum-deposited metal electrode causing electrical shorting-out of the cells [15]. Figure 3 shows the current-voltage characteristics.

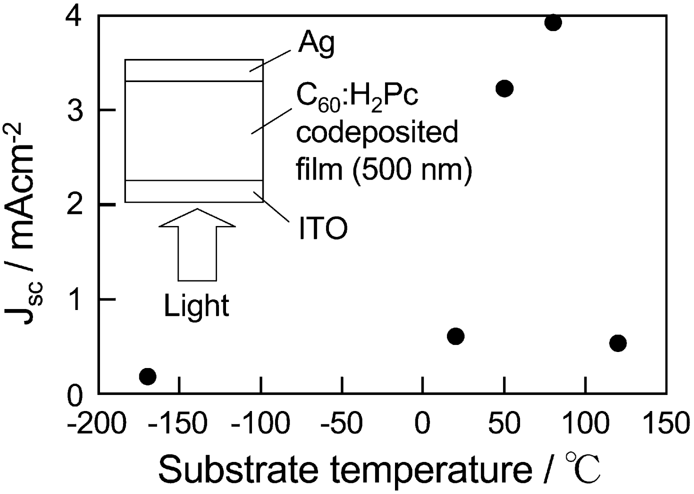

FIGURE 1 Dependence of J_{sc} of single-layered C_{60}:H_2Pc cells on substrate temperature during co-deposition. C_{60}:H_2Pc ratio was 1:1. Simulated solar light (92 mWcm^{-2}) was irradiated on the ITO electrode.

The best photovoltaic performance [J_{sc}: 9.9 mAcm^{-2}, V_{oc}: 0.42 V, FF: 0.52, photo-electric conversion efficiency: 2.5%] was observed when the thickness and the C_{60}:H_2Pc ratio of the co-deposited layer were optimized to 130 nm and 5:6, respectively. Figure 4 shows the spectral dependence of the internal quantum efficiency of J_{sc} (closed dots) and the absorption ratio of the incident light absorbed by the organic film (solid curve). The quantum efficiency is calculated as the ratio of the number of carriers collected under short-circuit conditions to the

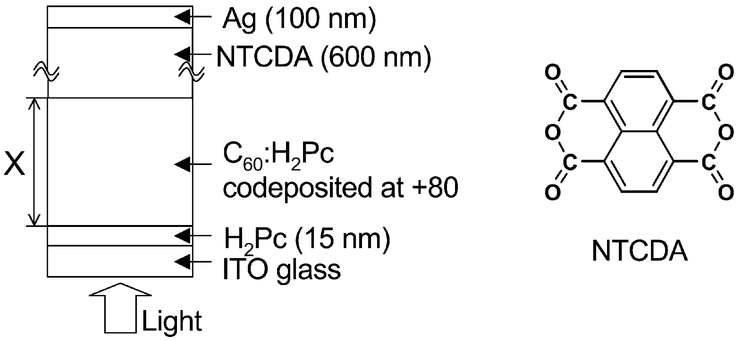

FIGURE 2 Three-layered cell. Chemical structure of NTCDA is also shown.

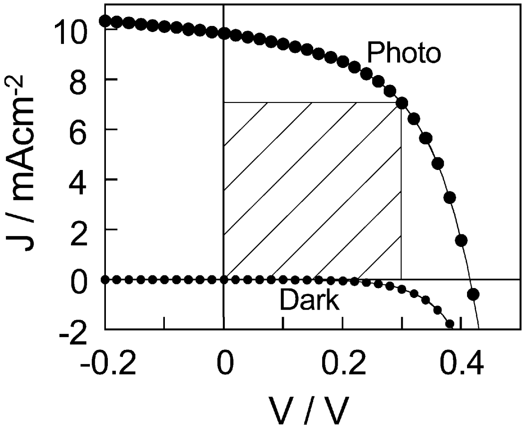

FIGURE 3 Current–voltage (J–V) characteristics of a three-layered cell incorporating a 130-nm-thick C_{60}:H_2Pc (5:6) interlayer co-deposited at +80°C. The shaded rectangle indicates the maximum power output. Performance; J_{sc}: 9.9 mAcm^{-2}, V_{oc}: 0.42 V, FF: 0.52, Efficiency: 2.5%. The intensity of simulated solar light transmitted through the ITO glass substrate was 85.8 mW cm^{-2}.

number of photons absorbed by the organic layers. Since the light transmitted through the C_{60}:H_2Pc (130 nm)/H_2Pc (15 nm) film is reflected by the Ag electrode and absorbed again by the same film, the absorption ratio for C_{60}:H_2Pc (260 nm)/H_2Pc (30 nm) film ought

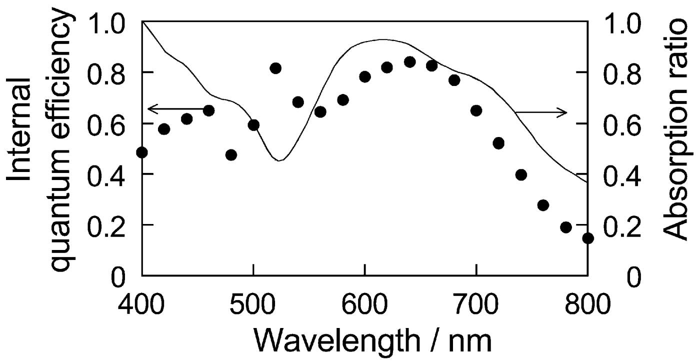

FIGURE 4 Spectral dependence of internal quantum efficiency of J_{sc} (closed dots) and absorption ratio of incident light by organic film (solid curve) for Figure 3 cell. The quantum efficiency is calculated as the ratio of the number of carriers collected under short-circuit conditions to the number of photons absorbed by the organic layers. Absorption ratio is calculated as the proportion of light intensity absorbed by organic layers to incident light intensity.

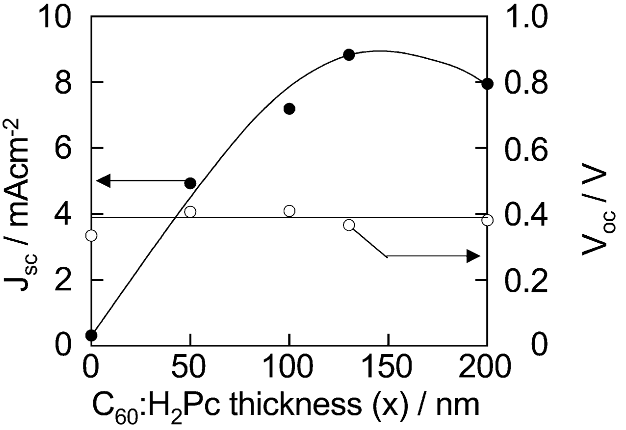

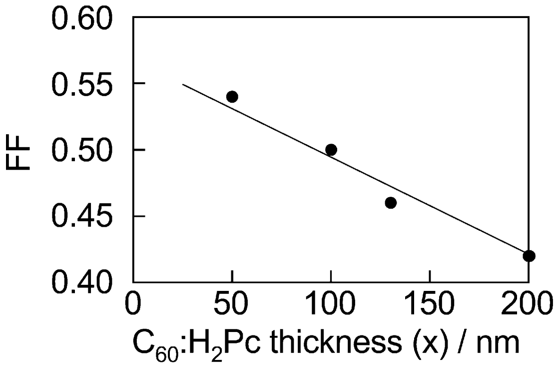

FIGURE 5 Dependence of J_{sc}, V_{oc}, and FF of the three-layered cells on C_{60}:H_2Pc thickness (x). C_{60}:H_2Pc ratio was 1:1.

to be used. The maximum and the averaged internal quantum efficiencies (400–800 nm) were 84% and 59.3%, respectively. Since there is hardly any indication of the existence of a masking effect in the relationship of the spectral shapes of the quantum efficiency and the absorption ratio, we concluded that the entire bulk of the 130 nm-thick co-deposited layer is active for photocurrent generation. From the solid curve in Figure 4, the total absorption ratio and the intensity absorbed by the organic layer for simulated solar light can be calculated as 53% (300–1100 nm) [16] and 45.5% mW cm^{-2}, respectively. Thus, the conversion efficiency with respect to absorbed solar light is calculated as 4.7%. Both the internal quantum efficiency and the absorption ratio (utilization efficiency of solar light) can stand further improvements.

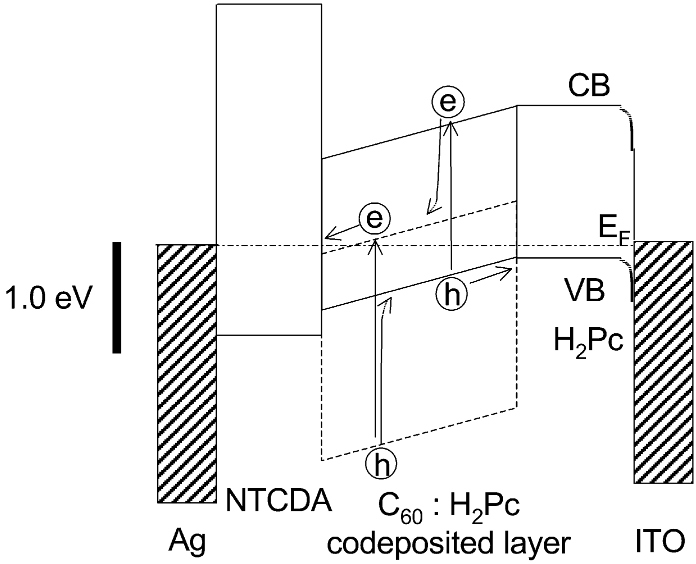

FIGURE 6 *p-i-n* energetic structure of the three-layered cell. The energetic relationships are precisely illustrated with respect to the scale bar. The valence band (VB) and the conduction band (CB) levels were estimated from the ionization potentials measured by atmospheric photoelectron emission analysis and from the optical band gaps. The C_{60} in the co-deposited layer is depicted using a broken line. E_F denote the Fermi level under the short-circuit condition.

Figure 5 shows the dependence of J_{sc}, V_{oc}, and FF of the three-layered cells (Fig. 2) on the thickness (x) of the C_{60}:H_2Pc. J_{sc} increased with increasing x up to 130 nm and then started to decrease. V_{oc} showed a constant value of approximately 0.4 V. FF decreased monotonically with increasing x. These characteristics can be reasonably explained based on a *p-i-n* energetic structure (Fig. 6). A built-in electric field, created by the difference in the Fermi levels (E_F) of NTCDA and H_2Pc, is distributed across the C_{60}:H_2Pc interlayer and drives efficient charge-carrier generation and charge transport in the co-deposited layer. The V_{oc} value of 0.4 V corresponds well with the built-in potential (0.4 V) estimated by the Kelvin-Zisman vibrating capacitor method [17]. The increase in J_{sc} between $x = 0$ nm and 130 nm is due to the increase in the absorption ratio of solar light induced by the C_{60}:H_2Pc interlayer. The decrease in J_{sc} above $x = 130$ nm is due to an increase in the resistance of the co-deposited layer with increasing x, which also causes a monotonic decrease in FF. Those observations support the *p-i-n* energetic structure. We

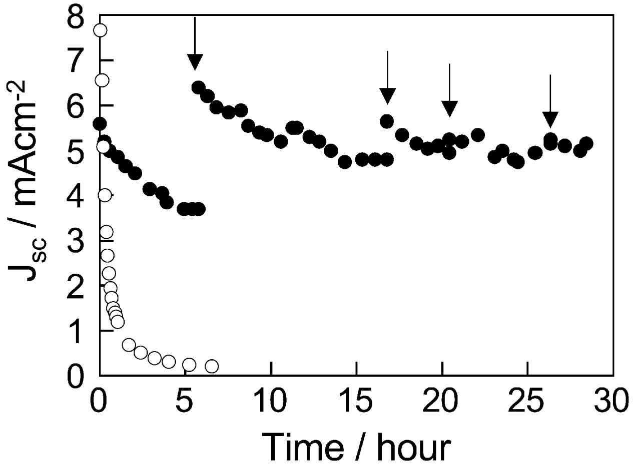

FIGURE 7 Dependence of J_{sc} on the cell operating time under vacuum condition of 0.1 Pa (closed dots) and in air (open dots). Light from halogen lamp (91 mWcm^{-2}) was irradiated under short-circuit condition. Cell structure was same to that of Figure 3. Arrows indicate the rest of the cell operation for about 12 hours under dark condition.

should point out the existence of a large energetic barrier for electron extraction from C_{60} to NTCDA. It is an unsolved question why such a large barrier does not deteriorate the cell performance. SEM observation of the cross section of NTCDA film revealed that there are no grain boundaries to the direction of electron transport. Thus, electrons photogenerated at co-deposited layer smoothly transport through NTCDA. Surprisingly, even if 2 μm-thick NTCDA was used, no suppression of cell performance was observed. We imagine that the π–π stacking is formed in the direction toward electrode. Thus, bulk resistance for electron transport in NTCDA is negligible.

The prolonged irradiation of the present cells with white light (91 mW cm^{-2}) was performed under short-circuit conditions (Fig. 7). A serious deterioration in the photocurrent of more than 90% was observed within 2 hours in air (open dots). However, this could be suppressed considerably under vacuum conditions (0.1 Pa) (closed dots) [18]. Therefore, for the long-term operation, cells should be isolated from air to avoid the ingress of oxygen or water.

CONCLUSION

p-i-n junction organic solar cells incorporating a nanostructure-optimized C_{60}:H_2Pc interlayer showed photo-electric conversion efficiencies of 2.5%. Following problems should be solved for further progress. (1) Low utilization efficiency for solar light, especially in the spectral regions between 400–500 nm and 700–1100 nm. (2) Small built-in potential due to the too-positive E_F of NTCDA, which is merely pseudo-*n*-type. *pn*-control by doping technique should be applied.

REFERENCES

[1] Spanggaard, H. & Krebs, F. C. (2004). *Solar Energy Materials & Solar Cells*, *83*, 125, and references therein.

[2] Hiramoto, M., Fujiwara, H., & Yokoyama, M. (1991). *Appl. Phys. Lett.*, *58*, 1062.

[3] Hiramoto, M., Fujiwara, H., & Yokoyama, M. (1992). *J. Appl. Phys.*, *72*, 3781.

[4] Hiramoto, M. (2005). In: *Organic Photovoltaics: Mechanisms, Materials and Devices*, Sun, S. & Sariciftci, N. S. (Eds.), CRC Press LLC: Boca Raton, Florida, Chapter 10, 239–270.

[5] Tang, C. W. (1986). *Appl. Phys. Lett.*, *48*, 183.

[6] Hiramoto, M., Suemori, K., & Yokoyama, M. (2002). *Jpn. J. Appl. Phys.*, *41*, 2763.

[7] Rostalski, J. & Meissner, D. (2000). *Solar Energy Materials & Solar Cells*, *61*, 87.

[8] Oishi, Y., Hiramoto, M., & Yokoyama, M. Extended Abstracts of the 48th Spring Meeting 2001, Japan Society of Applied Physics and Related Societies, 29a-ZG-7.

[9] Matsunobu, G., Oishi, Y., Yokoyama, M., & Hiramoto, M. (2002). *Appl. Phys. Lett.*, *81*, 1321.

[10] Gebeyehu, D., Maennig, B., Drechsel, J., Leo, K., & Pfeiffer, M. (2003). *Solar Energy Materials & Solar Cells*, *79*, 81.

[11] Sullivan, P., Heutz, S., Schultes, S. M., & Jones, T. S. (2004). *Appl. Phys. Lett.*, *84*, 1210.

[12] Uchida, S., Xue, J., Rand, B. P., & Forrest, S. R. (2004). *Appl. Phys. Lett.*, *84*, 4218.

[13] Furukawa, K., Terasaka, Y., Ueda, H., & Matsumura, M. (1997). *Synth. Metals*, *91*, 99.

[14] Suemori, K., Miyata, T., Hiramoto, M., & Yokoyama, M. (2004). *Jpn. J. Appl. Phys.*, *43*, L1014.

[15] Suemori, K., Miyata, T., Yokoyama, M., & Hiramoto, M. (2004). *Appl. Phys. Lett.*, *85*, 6269.

[16] This spectral region of absorption is based on that of crystal silicon solar cell.

[17] Saito, S., Soumura, T., & Maeda, T. (1984). *J. Vac. Soc. Technol.*, *A2*, 1389.

[18] For the plot of closed dots from 0 to 6 hours, incident light intensity lower than 91 $\mathrm{mWcm^{-2}}$ was used due to the technical reason.